

ORIGINAL ARTICLE

Rapid resonance Raman microspectroscopy to probe carbon dioxide fixation by single cells in microbial communities

Mengqiu Li¹, Daniel P Canniffe², Philip J Jackson^{2,3}, Paul A Davison^{1,2}, Simon FitzGerald⁴, Mark J Dickman³, J Grant Burgess⁵, C Neil Hunter² and Wei E Huang¹

¹Kroto Research Institute, Department of Civil and Structural Engineering, University of Sheffield, Sheffield, UK; ²Department of Molecular Biology and Biotechnology, University of Sheffield, Sheffield, UK; ³ChELSI Institute, Department of Chemical and Biological Engineering, University of Sheffield, Sheffield, UK; ⁴HORIBA Jobin Yvon Ltd, Middlesex, UK; ⁵School of Marine Science and Technology, and Centre for Bacterial Cell Biology, Newcastle University, Newcastle upon Tyne, UK

Photosynthetic microorganisms play crucial roles in aquatic ecosystems and are the major primary producers in global marine ecosystems. The discovery of new bacteria and microalgae that play key roles in CO₂ fixation is hampered by the lack of methods to identify hitherto-unculturable microorganisms. To overcome this problem we studied single microbial cells using stable-isotope probing (SIP) together with resonance Raman (RR) microspectroscopy of carotenoids, the light-absorbing pigments present in most photosynthetic microorganisms. We show that fixation of ¹³CO₂ into carotenoids produces a red shift in single-cell RR (SCRR) spectra and that this SCRR–SIP technique is sufficiently sensitive to detect as little as 10% of ¹³C incorporation. Mass spectrometry (MS) analysis of labelled cellular proteins verifies that the red shift in carotenoid SCRR spectra acts as a reporter of the ¹³C content of single cells. Millisecond Raman imaging of cells in mixed cultures and natural seawater samples was used to identify cells actively fixing CO₂, demonstrating that the SCRR–SIP is a noninvasive method for the rapid and quantitative detection of CO₂ fixation at the single cell level in a microbial community. The SCRR–SIP technique may provide a direct method for screening environmental samples, and could help to reveal the ecophysiology of hitherto-unculturable microorganisms, linking microbial species to their ecological function in the natural environment.

The ISME Journal (2012) 6, 875–885; doi:10.1038/ismej.2011.150; published online 24 November 2011

Subject Category: microbial ecology and functional diversity of natural habitats

Keywords: carbon dioxide fixation; Raman imaging; resonance Raman; single cell; carotenoids; photosynthesis

Introduction

Photosynthetic microorganisms including bacteria and algae are essential to aquatic life and the global carbon budget, but the precise ecological roles of many species remain ill defined because of cultivation difficulties which have led scientists to develop methods for detecting uncultured cells in the environment (Amann *et al.*, 1995; Venter *et al.*, 2004; Daniel, 2005). However, some uncultured photosynthetic bacteria and microalgae have been found to play crucial roles in carbon or nitrogen cycling (Weller *et al.*, 1992; Beja *et al.*, 2001; Karl, 2002;

Crump *et al.*, 2007; Stepanauskas and Sieracki, 2007; Zehr *et al.*, 2008; Tripp *et al.*, 2010). Recently, culture-independent approaches (for example, *in situ* hybridisation and 18S rRNA sequencing) have been employed to reveal two new groups of photosynthetic eukaryotes that play key roles in CO₂ fixation in the subtropical and tropical northeast Atlantic Ocean. These groups, Euk-A and Euk-B, have not yet been cultivated and, in the case of Euk-B, culture conditions for closely related species have never been defined (Jardillier *et al.*, 2010). It is reasonable to hypothesise that significant populations of uncultivated photosynthetic bacteria and algae remain to be discovered in the oceans. It is essential to monitor the photosynthetic activity of bacteria and algae including those hitherto-uncultivated microorganisms, and to understand their dynamic processes in relation to CO₂ fixation and climate change. In addition, uncultured oceanic photosynthetic bacteria and algae represent an

Correspondence: WE Huang, Kroto Research Institute, Department of Civil and Structural Engineering, North Campus, University of Sheffield, Sheffield, S3 7HQ, UK.
E-mail: w.huang@sheffield.ac.uk

Received 16 May 2011; revised 14 September 2011; accepted 14 September 2011; published online 24 November 2011

untapped biotechnological resource that could lead to discovery of new biomedical drugs and biocatalysts (Bode and Muller, 2005; Fortman and Sherman, 2005; Lorenz and Eck, 2005). Therefore, it would be useful to develop a culture-independent tool to unravel both the ecological function of photosynthetic bacteria and algae *in situ*, and to reveal their roles in the natural environment in terms of their relative contribution to carbon fixation.

Raman microspectroscopy has been shown to be a useful tool to study microbial cells (Huang *et al.*, 2004, 2007a, b, 2009a, b, 2010; Wagner, 2009; Haider *et al.*, 2010; Hall *et al.*, 2011; Wu *et al.*, 2011). In combination with other biological tools such as stable-isotope probing (SIP) and fluorescence *in situ* hybridisation, Raman single-cell technology can link bacterial species with their ecological roles without cultivation (Huang *et al.*, 2009a). Raman spectroscopy detects the vibrations of chemical bonds of molecules through the inelastic scattering of incident laser light (Huang *et al.*, 2010). Raman microspectroscopy is able to study single microorganisms and provide intrinsic cellular information (Huang *et al.*, 2004). A typical Raman spectrum contains a rich cellular chemical profile, including information on nucleic acids, protein, carbohydrates, lipids and pigments (for example, carotenoids), which enables the characterisation of different cell types, physiological and phenotypic changes to living cells (Huang *et al.*, 2004, 2007a, b, 2009a, 2010; Wagner, 2009; Haider *et al.*, 2010; Hall *et al.*, 2011). Raman imaging is a hyperspectral technique that can be used to acquire a full Raman spectrum at many hundreds or thousands of positions across a sample (for example, microorganisms on a microscopic slide). The resulting spectra can be interrogated to generate pseudo-colour images based on specific peaks of the Raman spectra. As these features relate to chemical entities within the sample, the Raman images can be used to illustrate the distribution of chemical components. Raman imaging would be desirable to 'visualise' chemical information of individual cells in a microbial community as it provides single-cell spatial resolution and a temporal dimension to study microbial identity and ecophysiology in complex microbial communities (Huang *et al.*, 2009a). However, the physical process of light scattering that underlies Raman spectroscopy is a rare event, with just one in 10⁶–10⁸ photons incident on the sample undergoing Raman scattering. Typically, the acquisition of a good-quality Raman spectrum from a single cell takes from several minutes to 4 s, making Raman imaging time consuming and hindering high-throughput screening and rapid imaging. Resonance Raman (RR) spectroscopy can enhance the Raman signal up to 10⁶-fold, which significantly reduces the acquisition time of Raman spectra (Robert, 2009). RR occurs when the frequency of incident light matches the electronic transition of the irradiated molecule. Many biologi-

cal molecules are RR-active compounds and carotenoids are typical analytes for RR spectroscopy (Krebs *et al.*, 2003; Robert 2009). More importantly, nearly all photosynthetic microorganisms contain carotenoids, which are essential elements of light-harvesting complexes and singlet oxygen quenchers (Szalontai *et al.*, 1994; Garcia-Asua *et al.*, 1998; Tracewell *et al.*, 2001, 2005).

In this study, we obtained single-cell RR (SCRR) spectra from carotenoid-containing bacteria and microalgae using short, milliseconds, acquisition times. SIP using ¹³C bicarbonate was employed to link bacterial species with their CO₂ fixation functions. The red shift of SCRR spectra (where Raman bands move to lower Raman shift or wave number position because of ¹³C labelling on the molecules; Huang *et al.*, 2004) was observed in photosynthetic microorganisms that had incorporated ¹³C bicarbonate into the cells. The results suggested that carotenoids were good biomarkers to indicate ¹³CO₂ incorporation in photosynthetic microorganisms with a sensitivity as low as 10% ¹³C content of single cells. Finally, we applied SCRR–SIP to generate Raman images that help *in situ* and quantitative identification of active ¹³CO₂-fixing microorganisms in culture mixtures and real seawater samples. This shows that SCRR–SIP may have great potential as a rapid *in situ* technique for imaging and screening of photosynthetic cells in natural microbial communities.

Materials and methods

Chemicals, media, strains and growth conditions

All chemicals used in this study were purchased from Sigma-Aldrich (Dorset, UK) unless otherwise stated. The ¹³C sodium bicarbonate contains 98 atom % ¹³C (catalogue number 372382). The microalgae strain AMA was isolated from Arctic supraglacial sites. *Synechocystis* sp. PCC 6803 and *Synechococcus elongatus* PCC 7942 were from our laboratory collection. Non-photosynthetic bacterial strains GWO, GWY and GWR with orange, yellow and red pigments, respectively, were isolated from contaminated groundwater in southwest United Kingdom (Huang *et al.*, 2009a). AMA, *Synechocystis* sp. PCC 6803 and *S. elongatus* PCC 7942 strains were grown in BG-11 media (Sigma-Aldrich) with various proportions of ¹²C and ¹³C sodium bicarbonate as the sole carbon source. To examine the integration of ¹³C in photosynthetic microorganisms, *Synechocystis* sp. PCC 6803 and *S. elongatus* PCC 7942 strains were grown in liquid BG-11 medium supplemented with different percentages of ¹³C bicarbonate. The final concentration of the total carbon source (¹²C and ¹³C bicarbonate) was 5 mM. Different ¹³C contents were achieved by mixing 1 M filter-sterilised ¹²C and ¹³C sodium bicarbonate solutions in appropriate ratios before adding to the BG-11 media. Bacterial

strains GWO, GWY and GWR were grown and maintained in R2A agar medium (Oxoid, UK).

Seawater was sampled from the coast at the Dove Marine Laboratory, Cullercoats, England. Photosynthetic organisms in the seawater samples were maintained in glass tanks under open air conditions near (<50 m) to the sampling point for several months. Original sea water was used to maintain the resulting natural photosynthetic microorganisms.

Microcosm setup for cyanobacterial cultures

To eliminate CO₂ from the culture vessel, a degasification step was done before the incubation in order to remove dissolved CO₂ in the BG-11 medium. This was achieved by boiling the BG-11 medium in a microwave oven for 1 min. Deionised water (10 ml) was added to the BG-11 medium to compensate for the loss of water during the degasification. A 0.45- μ m filter attached to a syringe filled with sodium hydroxide was linked to the bottle cap immediately after the degasification and the bottle cap was fastened (Supplementary Figure S1), and the medium was allowed to cool to room temperature. Pre-mixed ¹²C and ¹³C sodium bicarbonate solution and 50 μ l of cyanobacterial cell suspension (10⁸ per ml) were then added to the BG-11 medium by quickly opening the cap and re-sealing the bottle with a closed cap. *Synechocystis* sp. PCC 6803 was grown in media with ¹³C contents of 1.1% (¹³C natural abundance), 10.8%, 25.3%, 49.6%, 73.8% and 98%. *S. elongatus* PCC 7942 was grown in media supplemented with ¹³C contents of 1.1% (natural abundance), 49.6% and 98%. These ¹³C contents are corrected by taking account of ¹³C natural abundance and the 98% ¹³C bicarbonate used in the study. The culture vessel was incubated at 30 °C and 50 μ mol photons m⁻² s⁻¹ in an orbital shaker and agitated at 150 r.p.m. for 4 days (Innova 44 illuminated rotary incubator, New Brunswick Scientific, Cambridge, UK).

Incubation of seawater samples

A total of 30 ml of the sea water was sampled and ¹³C-NaHCO₃ was added into the seawater samples with a final concentration of 2 mM. The seawater samples were incubated in closed bottles at room temperature (20 °C) for 8 days with natural light. Control seawater samples were incubated with 2 mM ¹²C-NaHCO₃ under the same conditions.

Raman microspectroscopy analysis

Cells were sampled from microcosms and were washed with deionised water before analysing them with the Raman microscope. Each cellular suspension (5–10 μ l) was spread on a calcium fluoride (CaF₂) slide and allowed to air dry before Raman analysis. The SCRR spectra were acquired using a confocal Raman microscope (LabRAM HR, HORIBA

Scientific, London, UK) equipped with an integrated Olympus microscope (model BX41). A \times 100 magnifying dry objective (NA = 0.90, Olympus, Essex, UK) was used to observe and acquire Raman signals from single cells. The laser beam was targeted on the cell visually using an integrated colour camera and a motorised XYZ stage (0.1 μ m step). The Raman scattering was excited with a 532-nm Nd:YAG laser (Torus Laser, Laser Quantum, Manchester, UK). The laser power on a single cell was \sim 3.5 mW. The detector was a -70 °C air-cooled charge-coupled device detector (Andor, Belfast, UK). The system was run with a confocal pinhole diameter of 100 μ m, enabling a spatial resolution of \sim 1 μ m to be obtained. Each Raman spectrum was acquired between the range 2172 and 557 cm⁻¹, with 1021 data points and resolution of 1–1.5 cm⁻¹. LabSpec software (HORIBA Scientific) was used to control the Raman system and acquire Raman spectra. Acquisition times for SCRR spectra were 100 ms for single-cell measurements and 1–30 ms for Raman imaging. To each pure or mixed culture samples, 20 single cells were randomly chosen and measured. Pure β -carotene (Sigma Aldrich) was used as a carotenoid control and was measured under the same condition as SCRR.

Raman imaging

SWIFT (HORIBA Scientific) imaging function was coupled into the Raman systems, which allows significant reduction in the time needed for generating Raman images when very short spectral acquisition time is used (milliseconds in this study). In contrast to traditional start–stop mapping methods where the minimum measurement time is typically 500 ms per point, samples are continuously scanned beneath the laser beam, and spectra are acquired ‘on the fly’ as the sample is scanned in the SWIFT mode. SWIFT was employed to generate Raman images of photosynthetic bacterial populations in which the cells had different ¹³C contents. Three half–half mixed cyanobacterial cultures were imaged by SWIFT: (1) *Synechocystis* sp. PCC 6803 cells grown in 73.8% ¹³C bicarbonate BG-11 medium mixed with cells grown in ¹²C bicarbonate BG-11 medium; (2) *Synechocystis* sp. PCC 6803 cells grown in 10.8% ¹³C bicarbonate BG-11 medium mixed with cells grown in ¹²C bicarbonate BG-11 medium; and (3) *Synechocystis* sp. PCC 6803 cells grown in 10.8% ¹³C bicarbonate BG-11 medium mixed with *S. elongatus* PCC 7942 grown in ¹²C bicarbonate BG-11 medium. SWIFT was also used to image the seawater samples incubated with ¹³C-NaHCO₃ and ¹²C-NaHCO₃ to visualise the ¹³C-incorporated photosynthetic cells. Each Raman images was acquired within minutes and the acquisition time of each pixel was 1 ms for mixed cultures, and 10–30 ms for the seawater samples. A diffraction limited spatial resolution of \sim 0.7 μ m and a mechanical step of 0.5 μ m (4 million pixels mm⁻²) were used to generate the Raman images for cyanobacteria culture

mixtures; a mechanism step of 1 µm was used for the seawater sample. Raman images were analysed with LabSpec (HORIBA Scientific), and were generated by classical least squares modelling of hyperspectral data sets. At each image pixel position a linear combination of factors was calculated to estimate the measured spectrum, such that

$$I_i = \sum_{k=1}^l a_{ik} A_k + \varepsilon_i$$

where I_i is the i th measured spectrum of the data set, A_k is the k th loading input to the calculation, a_{ij} is the score of the spectrum I_i with respect to the loading A_k , $a_{ij}A_k$ is a factor and ε_i is the error between the spectrum (measurement) I_i and the estimation

$$\sum_{k=1}^l a_{ik} A_k.$$

Loading spectra (A_k) were selected by averaging spectra from manually selected regions of interest within the data set. The images display scores (a_{ik}) as a function of x axis and y axis positions. The green or yellow colour in the Raman images indicated the ¹²C carotenoids in cells, whereas the red colour indicated the ¹³C carotenoids in cells (characterised by the red shifted RR peaks). In the Raman images of seawater samples, the purple colour was defined as the fluorescence because some organisms with autofluorescence were observed, which appeared as a broad, featureless spectrum without the expected sharper RR peaks.

Raman spectra analysis

All Raman spectra were recorded, smoothed and baseline corrected using LabSpec. Spectra smoothing was performed by the Savitsky–Golay smoothing method. Positions of the SCRR bands were determined using LabSpec and were subsequently imported to SPSS 15 (IBM Corporation, New York, NY, USA) for further analysis. The positions of SCRR Raman bands of *Synechocystis* sp. PCC 6803 and *S. elongatus* PCC 7942 were analysed statistically to establish a relationship between the extent of red shift and ¹³C content in cells. The wave numbers of the Raman bands were plotted against the ¹³C contents, with the error bars and linear regression lines (SPSS 15). Two-sample t -tests were performed in SPSS between the ¹²C and 10.8 % ¹³C PCC6803 samples on three major bands of SCRR. MVSP 3.13g (Kovach Computing Services, Pantraeth, UK) was used to perform principal component analysis for SCRR spectra.

Absorbance analysis of *Synechocystis* sp. PCC 6803

A total of 5 ml of *Synechocystis* sp. PCC 6803 was harvested by centrifugation (Eppendorf, Cambridge, UK) at 3000 r.p.m. for 5 min. The cells were then re-suspended in the same volume of phosphate

buffer solution. To obtain a light absorbance spectrum of *Synechocystis* sp. PCC 6803, 200 µl of cells was scanned in the visible range using a microplate reader (Synergy 2, BioTek, Potton, UK). The absorbance spectrum was recorded in triplicate with a spectral resolution of 5 nm in the range of 400 nm to 750 nm.

Mass spectrometry (MS) analysis of ¹³C content of *Synechocystis* sp. PCC 6803 proteins

Batches of *Synechocystis* sp. PCC 6803 cells were grown in BG-11 media with different percentages of ¹³C-NaHCO₃ (1.1%, 10.8%, 49.6% and 98%) as the sole carbon source. The growth conditions were the same as described above. After 4 days of growth, 5 ml of each culture were sampled for single-cell Raman spectroscopy analysis. Meanwhile, 10 ml of each culture were taken and the cells were harvested by centrifugation at 4000 r.p.m. for 10 min. Cells from each *Synechocystis* sp. PCC 6803 sample were re-suspended in 0.2 ml of SDS sample buffer containing tracker dye and 0.05% (v/v) mercaptoethanol (Sigma, Poole, UK). After incubation at 90 °C for 10 min, 15 µl was applied to a NuPAGE Bis-Tris gel (1.0 mm, 12%; Invitrogen, Paisley, UK) according to the manufacturer's protocol. The gel was stained with colloidal Coomassie Blue (Bio-Rad Laboratories, Hemel Hempstead, UK) and the same prominent protein band (at 50–75 kDa) excised from the four lanes (Supplementary Figure S2). The bands were subjected to in-gel tryptic digestion according to Pandey *et al.* (2000).

The extracted peptides were separated on an UltiMate 3000 nanoflow liquid chromatography system (Dionex, Camberley, UK) using 5 mm × 300 µm (trapping) and 150 mm × 75 µm (analytical) PepMap C₁₈ reverse-phase columns (Dionex). Linear gradient elution was from 97% solvent A (0.1% formic acid in 3% acetonitrile) to 35% solvent B (0.1% formic acid in 97% acetonitrile) at a flow rate of 300 nl min⁻¹ for 40 min. On-line MS was done on a Maxis UHR-TOF (Bruker Daltonics, Coventry, UK) using profile MS with automatic dependent tandem mass spectrometry (MS/MS) data acquisition.

The nano liquid chromatography–MS/MS data file corresponding to the incorporation experiment at natural isotopic abundance was used as input for database searching (Mascot software supplied by Matrix Science, London, UK) to identify the protein band and its component tryptic peptides. The ¹³C incorporation ratios in the samples were determined by comparison of the observed isotope distribution pattern of the representative peptide with the theoretical isotope distribution pattern generated using IsoPro v3.1 (<http://sites.google.com/site/isoproms>).

Results

Cells containing carotenoids display strong RR effects

The absorption spectrum of *Synechocystis* sp. PCC 6803 in the visible range showed peaks at 440, 620

and 670 nm (Supplementary Figure S3). Carotenoids absorb light in the 400–550 nm range (Gust *et al.*, 1993), and the 532 nm laser for Raman excitation used in this study preferentially excites the carotenoids rather than the chlorophyll pigments.

RR spectra of carotenoid molecules display characteristic Raman bands: ν_1 , ν_2 and ν_3 (Figure 1, β -carotene spectrum). The sharp and strong ν_1 (stretching mode of the C=C bonds at ~ 1515 cm⁻¹), ν_2 (stretching mode of the C-C bonds at ~ 1155 cm⁻¹) and ν_3 (deformation of the methyl groups at ~ 1003 cm⁻¹) peaks can be unambiguously assigned to carotenoids (Rimai *et al.*, 1973; Tracewell *et al.*, 2001; Robert, 2009). The position of the ν_1 band varies according to the length of the conjugated C=C bond chain (Rimai *et al.*, 1973; Carey, 1978; Tracewell *et al.*, 2001; Robert, 2009). The ν_2 band varies depending on the molecular conformation, and the ν_3 band is related to carotenoid methyl groups (Rimai *et al.*, 1973; Carey, 1978; Tracewell *et al.*, 2001; Robert, 2009). The RR signals of carotenoids are so strong that with 532 nm laser excitation the SCRR spectra of carotenoid-containing microorganisms predominantly display the ν_1 , ν_2 and ν_3 Raman bands, which in Figure 1 arise from the typical carotenoid β -carotene. The positions of the ν_1 band in particular varied significantly among the various microorganisms studied, with the ν_2 and ν_3 bands also affected to a lesser extent (Figure 1). We noted a variation of 17.2, 1.7 and 4.9 cm⁻¹ at the ν_1 , ν_2 and ν_3 positions, respectively, which arose from the different conformations and composition of the carotenoid molecules within the cells.

The red shift of SCRR spectra due to ¹³C incorporation in cells

Figure 2 shows the SCRR spectra of *S. elongatus* PCC 7942 and *Synechocystis* sp. PCC 6803 grown in media supplemented with different proportions of ¹³C bicarbonate. The RR bands of both species displayed a red shift, the extent of which was dependent on the level of ¹³C bicarbonate in the growth medium. For *S. elongatus* PCC 7942, the ν_1 , ν_2 and ν_3 bands of ¹²C cells shifted from 1522.0, 1157.7 and 1006.0 cm⁻¹ to 1484.9, 1128.2 and 989.5 cm⁻¹, respectively, in ¹³C-labelled cells (Figure 2). For *Synechocystis* sp. PCC 6803, the ν_1 , ν_2 and ν_3 bands of ¹²C cells shifted from 1516.8, 1155.6 and 1004.3 cm⁻¹ to 1480.9, 1125.3 and 988.6 cm⁻¹, respectively, in ¹³C-labelled cells (Figure 2). Among the three dominant SCRR bands, the ν_1 band had the greatest (~ 36 cm⁻¹) and ν_3 band least (~ 16 cm⁻¹) red shift; and the ν_2 band had an intermediate ~ 30 cm⁻¹ red shift (Table 1) in the range of 1.1–98% ¹³C cells. This experiment encompasses the full range of labelling possible, considering that the natural abundance of ¹³C is 1.1% and the ¹³C content in Sigma-Aldrich ¹³C sodium bicarbonate is 98%.

Figure 3 shows that the extent of the red shift of the ν_1 , ν_2 and ν_3 Raman bands was proportional to the ¹³C content of the cells, suggesting that the spectral red shift can be used as a quantitative

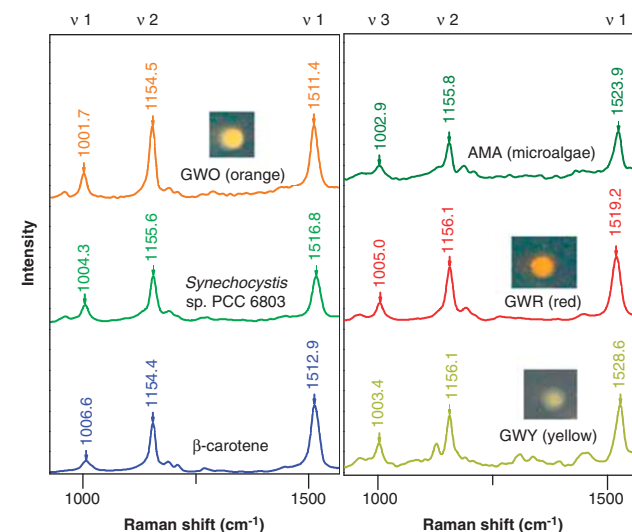


Figure 1 SCRR spectra of *Synechocystis* sp. PCC 6803, microalgae and bacteria with carotenoid pigments. The dominant Raman bands of SCRR spectra were from carotenoids, as shown by comparison with the spectrum of pure β -carotene.

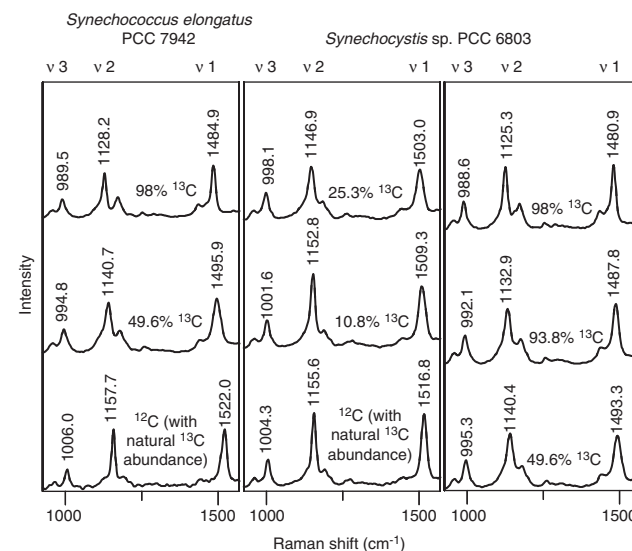


Figure 2 RR spectra of *S. elongatus* PCC 7942 and *Synechocystis* sp. PCC 6803 grown in media containing different percentages of ¹³C-NaHCO₃.

Table 1 Raman shift due to ¹³C incorporation (cm⁻¹)

Carotenoid bands	<i>Synechococcus elongatus</i> PCC 7942	<i>Synechocystis</i> sp. PCC 6803
ν_1	37.1	35.9
ν_2	29.5	30.3
ν_3	16.5	15.7

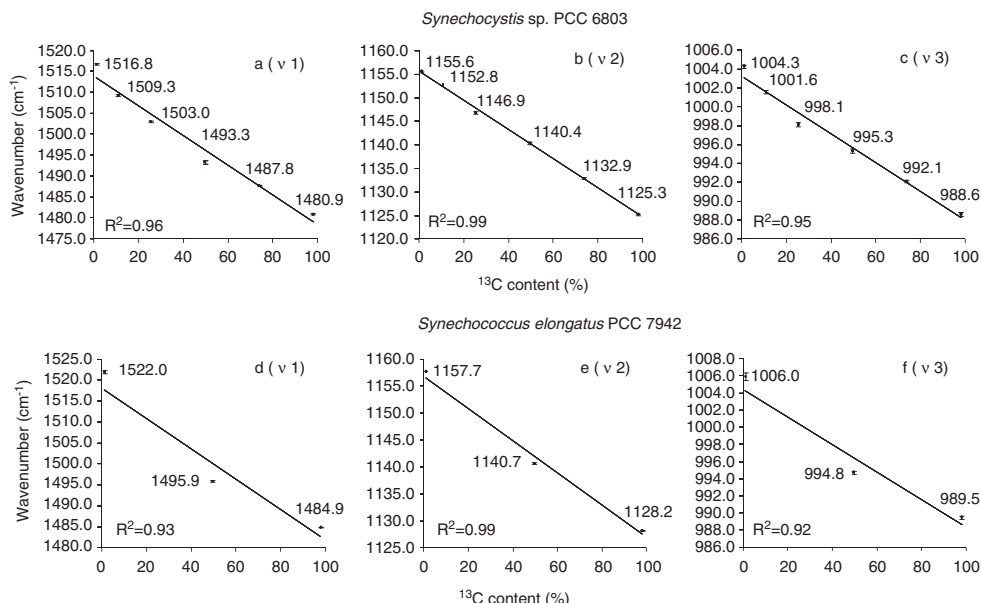


Figure 3 Linear regression of the ‘red shift’ of the v1 (a), v2 (b) and v3 (c) bands of the ¹³C-incorporated *Synechocystis* sp. PCC 6803 single cells and the v1 (d), v2 (e) and v3 (f) bands of the ¹³C-incorporated *S. elongatus* PCC 7942 single cells. On each sample, 20 replicates were performed.

biomarker for ¹³C incorporation. Linear regression of data obtained from 20 randomly chosen single cells from three biological replicates (Figure 3) demonstrate that the three Raman bands shift in a linear manner (linear regression $R^2 > 0.9$). It is notable that the red shifts of the *Synechocystis* sp. PCC 6803 bands show distinguishable differences between the ¹²C (containing natural abundance 1.1% ¹³C) and 10.8% ¹³C cells (Figure 3). The *t*-tests of the v1, v2 and v3 bands between the ¹²C and 10.8% ¹³C samples indicate that these differences were significant (P -values < 0.001). The slopes of the v1, v2 and v3 regression lines of *S. elongatus* PCC 7942 and *Synechocystis* sp. PCC 6803 are slightly different (Figure 3). However, for each cell type, the v1, v2 and v3 bands show a stepwise shift to lower energy wave numbers with increasing ¹³C content in cells (Figure 2 and Supplementary Figure S4), which makes it possible to establish a calibration to estimate the ¹³C content of a single cell based on its RR spectrum (Figure 3). The principal component analysis was carried out using the whole SCRR spectra and the results show the distinct separations among samples with different ¹³C contents (Supplementary Figure S5). The largest principal component analysis loadings at axes 1 and 2 were associated with the v1 and v2 bands, indicating that these spectral features are the most important factors for the classification of the SCRR spectra into different groups, as shown in Supplementary Figure S5.

MS analysis of the ¹³C incorporation in cells matches SCRR analysis

MS was applied to analyse ¹³C incorporation in *Synechocystis* sp. PCC 6803. MS analysis of

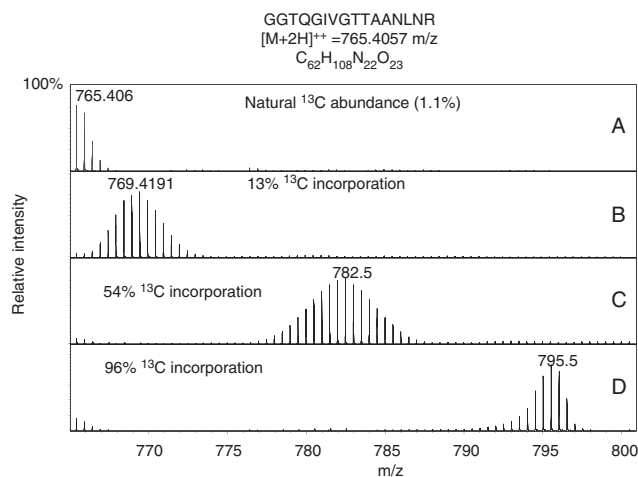


Figure 4 Mass spectra of peptide GGTQGVGTAAANLNR in protein Slr1841 of *Synechocystis* sp. PCC 6803 with different ¹³C incorporation ratios. The mass-charge ratios of the modal ions are labelled.

extracted proteins was used to determine the levels of ¹³C incorporation in cells. The MS spectra of a representative peptide GGTQGVGTAAANLNR $[M+2H]^{++}$ identified in protein Slr1841 of *Synechocystis* sp. PCC 6803 grown in 1.1%, 10.8%, 49.6% and 98% ¹³C is shown in Figure 4. The mass shift observed in the MS spectra is due to ¹³C incorporation in the peptide (Figure 4). The percentage of ¹³C incorporation was determined by comparison of the observed and theoretical isotope distribution pattern. The results show that the ¹³C incorporation in the peptide was 1.1%, 13%, 54% and 96%, respectively (Figure 4 and Supplementary

Figure S6). The SCRR spectral analysis of 20 single cells from each sample indicated that the corresponding samples contained, respectively, $1.1 \pm 0.4\%$, $9.4 \pm 0.5\%$, $51 \pm 0.7\%$ and $95 \pm 0.6\%$ of ¹³C incorporated in the cells of *Synechocystis* sp. PCC 6803 according to the calibration curves established in Figure 3. The results verify that the ¹³C contents of single cells measured by SCRR spectroscopy do indeed reflect the ¹³C-incorporation percentages in the whole cells measured by mass spectrometry.

Raman images differentiate cells with varying levels of ¹³C incorporation

To demonstrate the potential of RR spectroscopy as an *in situ* 'biochemical' imaging technique for photosynthetic microorganisms, two-dimensional Raman imaging was carried out on the three different cyanobacterial cell mixtures described in the Materials and Methods section (Figure 5). The spectra shown in Figure 5 are SCRR spectra taken at the centre of the circled cells with a 1-ms acquisition

time. The optical images matched well with the pseudocolour Raman images, as the green colour and the red/yellow colour indicate the locations of ¹²C- and ¹³C-incorporated single cells, respectively (Figure 5). The intensity of pseudocolour is proportional to the intensity of the Raman bands. Figure 5a shows a clear difference between ¹²C- and 73.8% ¹³C-incorporated cells. The SCRR-based Raman images were so sensitive that they were able to distinguish a subtle difference in the cells with 1.1% and 10.8% ¹³C incorporation (Figure 5b and c). As shown in Figure 5c, the Raman image of the cells based on RR spectra is consistent with the known morphology of rod-like *S. elongatus* PCC 7942 cells and spherical *Synechocystis* sp. PCC 6803 cells.

Figure 6 shows that Raman images can be used to distinguish ¹³C-labelled microorganisms at the single cell level within a complex microbial community in real seawater samples. The sample incubated with ¹²C-NaHCO₃ provided a baseline for the SCRR spectra used to estimate ¹³C incorporation of diverse photosynthetic microorganisms (Figure 6a). The Raman

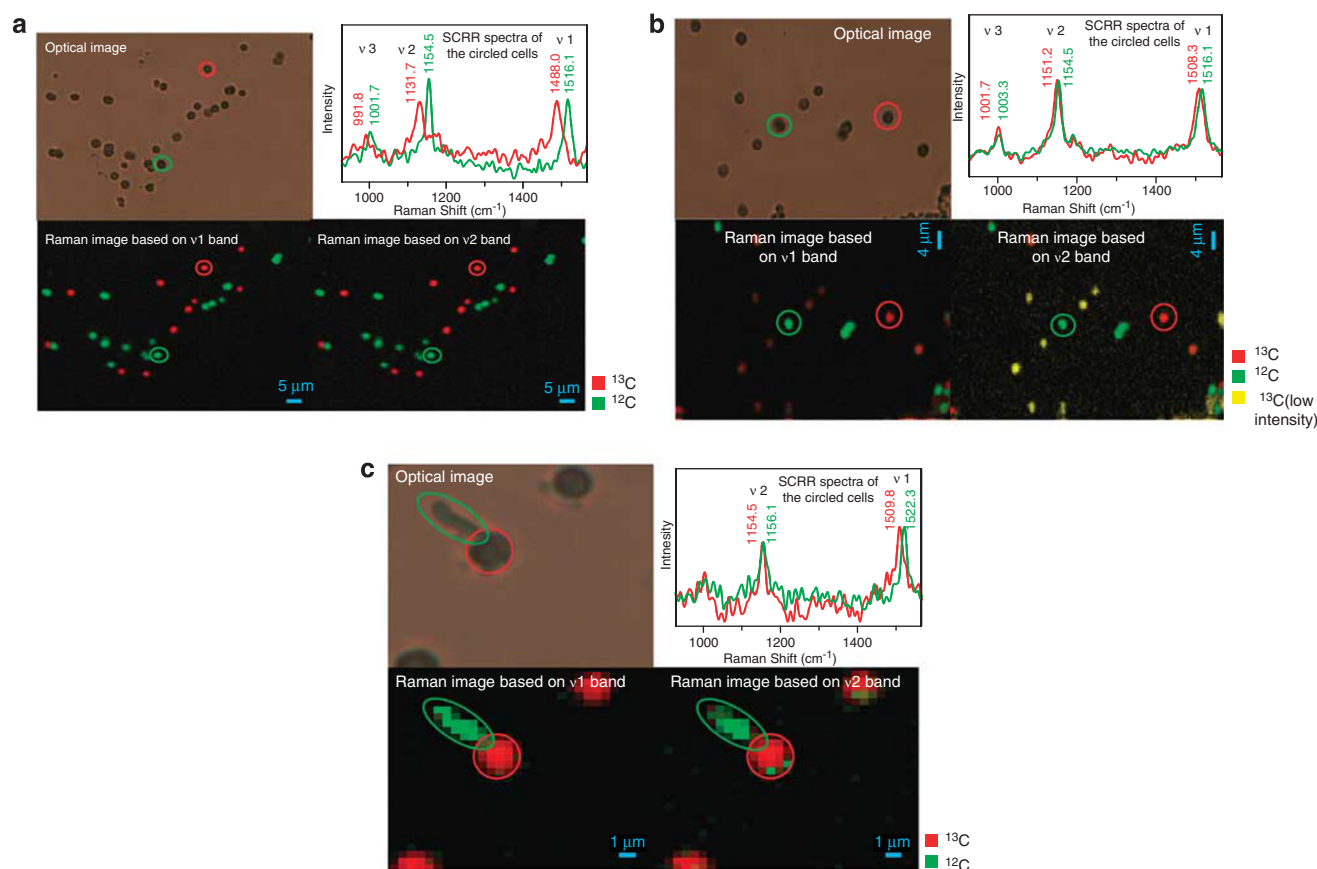


Figure 5 Raman images of mixed cell cultures with different ¹³C contents: (a) *Synechocystis* sp. PCC 6803 grown in BG11 medium supplemented with 73.8% ¹³C-NaHCO₃ mixed with the same species grown in BG11 medium supplemented with ¹²C-NaHCO₃. (b) *Synechocystis* sp. PCC 6803 grown in BG11 medium supplemented with 10.8% ¹³C-NaHCO₃ mixed with the same species grown in BG11 medium supplemented with ¹²C-NaHCO₃. (c) *Synechocystis* sp. PCC 6803 grown in BG11 medium supplemented with 10.8% ¹³C-NaHCO₃ mixed with *S. elongatus* PCC 7942 grown in BG11 medium supplemented with ¹²C-NaHCO₃. Two Raman images were generated based on the v1 and v2 bands. The ¹³C-incorporated single cells are displayed in red and the ¹²C cells green. Some ¹³C-incorporated cells with lower signal strength are displayed in yellow. The SCRR spectra are coloured to correspond to the ¹³C-labelled cells and ¹²C cells indicated by red and green circles, respectively.

images in Figures 6b and c suggest that after 8 days of incubation with ¹³C-NaHCO₃, some species have started to incorporate ¹³C into their cell components. The Raman imaging results show that cells, tentatively identified as the microalgal *Tetraselmis sp.* (cells 1b and 2b in Figure 6b and cell 2c in Figure 6c) and the diatom *Phaeodactylum tricornutum* (cell 4c, a tip of this triradiate-shaped microorganism in Figure 6c) were actively fixing ¹³C-NaHCO₃ whereas one possible photosynthetic species (cell 3b in Figure 6b) was present but incorporated little ¹³C-NaHCO₃ into the cells.

Tetraselmis sp. and *Phaeodactylum tricornutum* in the samples were identified by Zhang (2011). Figure 6c shows that at least four different species demonstrated ¹³C incorporation: *Tetraselmis sp.*, *Phaeodactylum tricornutum* and unidentified rod-shaped cells 1c and 3c, which show a red shift of RR bands in comparison with control cells grown in sea water with ¹²C-NaHCO₃. Based on the red shift of the RR bands as shown in Figure 6b (cells 1 and 2) and Figure 6c (cell 2), *Tetraselmis sp.* is estimated to incorporate ~20% ¹³C into cellular compounds after 8 days of incubation.

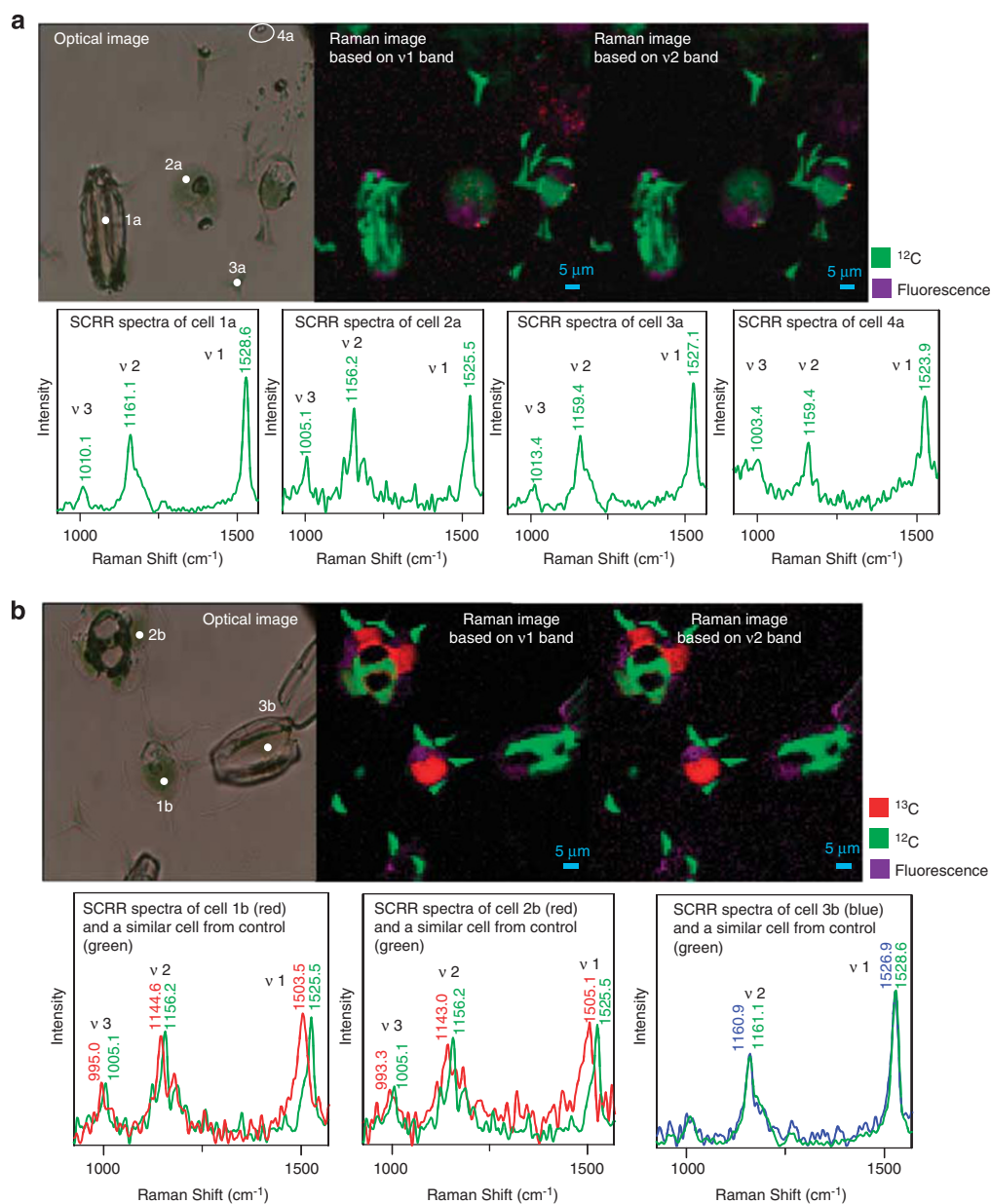


Figure 6 Raman images of the seawater sample that was grown in original sea water supplemented with 2 mM ¹²C-NaHCO₃ (**a**) and 2 mM ¹³C-NaHCO₃ (**b**, **c**). Two Raman images were generated based on the v1 and v2 bands. The ¹³C-incorporated single cells are displayed in red. The purple colour indicates the fluorescent region of the cells. SCRR spectra corresponding to the marked cells are shown.

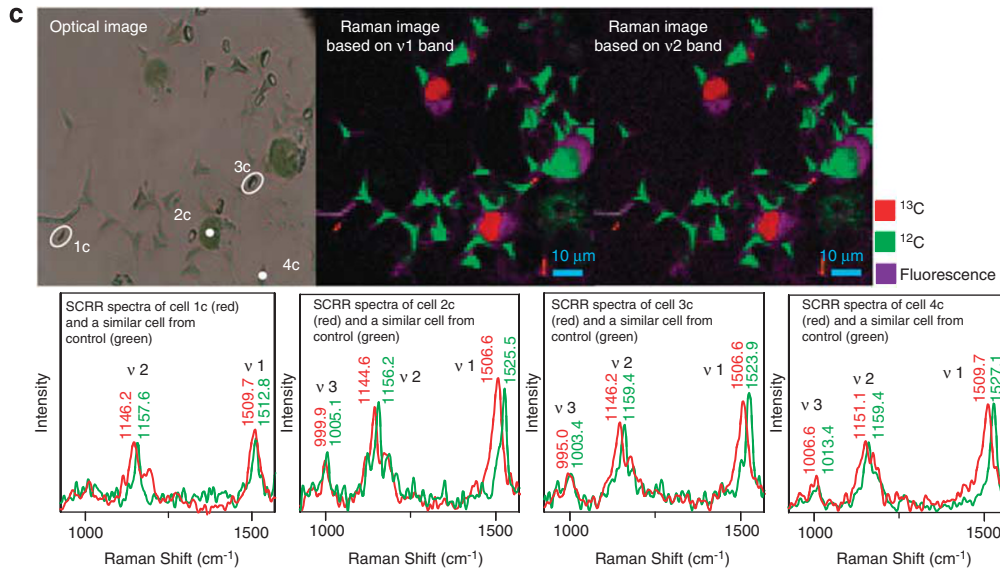


Figure 6 Continued.

Discussion

Raman spectra from single cells can be used as intrinsic ‘fingerprint’ without invasive labelling (Huang *et al.*, 2004, 2007a, b, 2009a, 2010; Wagner, 2009; Haider *et al.*, 2010; Hall *et al.*, 2011). However, the broad application of Raman spectroscopy in environmental microbiology is hindered by the naturally weak Raman effect. This study has demonstrated that by using carotenoids as internal biomarkers, SCRR combined with SIP can distinguish and image CO₂-fixing cells on a millisecond timescale. This method is also suitable for *in situ* identification and imaging of CO₂-fixing photosynthetic microorganisms in a quantitative manner (Figures 4 and 5).

As a 532 nm laser was chosen to record SCRR spectra from carotenoid-containing cells, the Raman acquisition time for a single cell was reduced to the millisecond level. This rapid Raman detection method paves the way for the development of a Raman cell sorter that could be a vital tool for metabolic analysis of high numbers of environmentally derived uncultured cells.

Cyanobacteria are the largest, most diverse and widely distributed group of photosynthetic prokaryotes (Stanier and Cohenbazire, 1977). In this study, *S. elongatus* PCC 7942 and *Synechocystis* sp. PCC 6803 were used as model photosynthetic microorganisms to test the SCRR–SIP methodology and using carbon dioxide fixation as an example of the study of an important eco-physiological property. SCRR–SIP was applied to identify microorganisms actively fixing CO₂ in real seawater samples (Figure 6), confirming that this technique could be used to identify and isolate key photosynthetic microorganisms that carry out CO₂ fixation in aquatic environments.

In order to establish a reliable quantitative measurement of the ¹³C content of photosynthetic microorganisms based on the red shift of SCRR, it was essential to grow cyanobacterial strains in conditions that minimise the effect of atmospheric CO₂. Preliminary data showed that *Synechocystis* sp. PCC 6803 appears to prefer CO₂ dissolved from the air rather than ¹³C bicarbonate in the growth medium. To eliminate any potential influence of CO₂ from atmosphere, the procedure described in this study was used.

SIP is a method widely used to study carbon and nitrogen flow in ecosystems. Introducing stable isotope compounds into an environmental sample allows researchers to determine which organisms incorporate the substrates of interest. Both mass spectra and vibrational spectra can be used in combination with SIP for work on single cells. In terms of sensitivity, spatial resolution and quantitative detection, mass spectra-based methods such as secondary ion mass spectrometry are superior over those based on vibrational spectra such as Raman spectroscopy. However, SCRR is a noninvasive method and provides molecular profiles or ‘fingerprints’ of cells, whereas secondary ion mass spectrometry is an invasive technology and detects atoms and small ions but not molecules (Wagner, 2009). Nucleic acid-SIP is an effective method for revealing microbial ecological functions in native environments (Radajewski *et al.*, 2000; Manefield *et al.*, 2002; Dumont and Murrell, 2005; Huang *et al.*, 2009a; Chen and Murrell, 2010). It usually employs equilibrium density gradient centrifugation to separate ¹³C-containing nucleic acids and the analysis of the separated nucleic acids links the function of microorganisms to their taxonomic identities (Radajewski *et al.*, 2000; Manefield *et al.*, 2002; Dumont and Murrell, 2005; Huang *et al.*, 2009a;

Chen and Murrell, 2010). Because of the subtle differences in the physical properties between stable isotopes, it would be a challenge to use the centrifugation-based SIP method for the isolation of ¹³C-incorporated DNA or RNA if ¹³C incorporation was <50%. In this study, we have demonstrated that SCRR-SIP is sufficiently sensitive to distinguish between cells with only 10% ¹³C incorporation and their cells containing ¹³C at the natural 1.1% abundance (Figures 3, 4 and Supplementary Figure S4). Applying the SCRR-SIP technique to real environmental samples also demonstrates that it is able to identify photosynthetic cells with only ~20% ¹³C content in their cellular compounds (Figure 6). Such a high sensitivity suggests that this technique may be useful in several applications: (1) detection of ¹³C-incorporated single microbial cells, avoiding the cross-feeding problem in SIP and aiding identification of the species that fix CO₂; and (2) observation of the temporal dynamics of the ¹³C incorporation in different species by taking SCRR spectra or Raman images at different times of the incubation. In *Synechocystis*, the measured red shifts in the ν_1 and ν_2 bands at 0% and 10% ¹³C incorporation were 7.5 and 2.8 cm⁻¹, respectively, indicating that SCRR-SIP may be able to detect ¹³C incorporation at levels even <10%. SCRR-SIP is a noninvasive technique, enabling the recovery of cells after measurement, which is especially useful for the study of unculturable microorganisms. For example, the two unknown rod-shaped bacteria identified in Figure 6c appeared to fix CO₂ but so far they have not been cultured, and further work is needed to confirm their photosynthetic ability. In certain habitats, a few species of non-photosynthetic obligate chemolithotrophic bacteria that also contain carotenoids have been reported, though these types of bacteria appear to be rare. In marine ecosystems, it is also increasingly clear that non-photosynthetic autotrophic bacteria are widespread in, for example, oxygen minimum zones. Thus, it is also possible that autotrophic non-photosynthetic bacteria exist, and, interestingly, could be detected by this approach if used in future studies. The ν_2 Raman bands appeared to vary in a narrower range (usually a few wave numbers) in different species, making it a potential biomarker for ¹³C incorporation in unidentified photosynthetic microorganisms. However, for samples that consist of various unknown species, the error of detection of ¹³C incorporation can be raised because of the uncertainty in the positions of the RR bands; therefore affecting the estimation of ¹³C-incorporation ratios. This indicates that a further investigation of the variation of ν_2 Raman bands in different carotenoid-containing cells is required.

To search and screen large numbers of single cells from environmental samples, a rapid Raman imaging technique has great potential. Taking Figure 5a as an example, a 90.5 × 74.7 μm Raman image that consists of 27 000 Raman spectra/pixels was generated in ~5 min with 1 ms acquisition time per pixel.

If we assume a grid of 2 μm × 2 μm contains a single cell, 10 000 single cells can be mapped in ~30 min. The Raman imaging time can be further reduced by using a more powerful computer, an optimised charge-coupled device detector and a refined spectrum readout strategy. It may also be possible to combine a laser microdissection system with this technique to selectively dissect and collect microorganisms of interest at the single cell level for attempted cultivation, genomic amplification and sequencing. In such a way, Raman imaging may provide a direct screening method for environmental samples without cultivation, and could help to reveal the precise ecological role of the 'black box' (unculturable microorganisms) in the microbial world.

Acknowledgements

We thank the University of Sheffield for providing a studentship to ML. We also thank Dr Jinwei Zhang at Newcastle University for supporting the seawater sampling. WEH and MJD thank support from the Engineering and Physical Sciences Research Council (EPSRC). DPC, PJJ, MJD and CNH would like to acknowledge financial support from the Biotechnology and Biological Sciences Research Council (UK). JGB thanks the NERC for financial support.

References

- Amann RI, Ludwig W, Schleifer KH. (1995). Phylogenetic identification and in-situ detection of individual microbial-cells without cultivation. *Microbiol Rev* **59**: 143–169.
- Beja O, Spudich EN, Spudich JL, Leclerc M, DeLong EF. (2001). Proteorhodopsin phototrophy in the ocean. *Nature* **411**: 786–789.
- Bode HB, Muller R. (2005). The impact of bacterial genomics on natural product research. *Angew Chem Int Ed* **44**: 6828–6846.
- Carey PR. (1978). Resonance Raman-spectroscopy in biochemistry and biology. *Q Rev Biophys* **11**: 309–370.
- Chen Y, Murrell JC. (2010). When metagenomics meets stable-isotope probing: progress and perspectives. *Trends Microbiol* **18**: 157–163.
- Crump BC, Peranteau C, Beckingham B, Cornwell JC. (2007). Respiratory succession and community succession of bacterioplankton in seasonally anoxic estuarine waters. *Appl Environ Microbiol* **73**: 6802–6810.
- Daniel R. (2005). The metagenomics of soil. *Nat Rev Microbiol* **3**: 470–478.
- Dumont MG, Murrell JC. (2005). Stable isotope probing - linking microbial identity to function. *Nat Rev Microbiol* **3**: 499–504.
- Fortman JL, Sherman DH. (2005). Utilizing the power of microbial genetics to bridge the gap between the promise and the application of marine natural products. *ChemBiochem* **6**: 960–978.
- Garcia-Asua G, Lang HP, Cogdell RJ, Hunter CN. (1998). Carotenoid diversity: a modular role for the phytoene desaturase step. *Trends Plant Sci* **3**: 445–449.

- Gust D, Moore TA, Moore AL, Jori G, Reddi E. (1993). The photochemistry of carotenoids - some photosynthetic and photomedical aspects. *Ann NY Acad Sci* **691**: 32–47.
- Haider S, Wagner M, Schmid MC, Sixt BS, Christian JG, Hacker G *et al.* (2010). Raman microspectroscopy reveals long-term extracellular activity of chlamydiae. *Mol Microbiol* **77**: 687–700.
- Hall EK, Singer GA, Polzl M, Hämmerle L, Schwarz C, Daims H *et al.* (2011). Looking inside the box: using Raman microspectroscopy to deconstruct microbial biomass stoichiometry one cell at a time. *ISME J* **5**: 196–208.
- Huang WE, Bailey MJ, Thompson IP, Whiteley AS, Spiers AJ. (2007a). Single-cell Raman spectral profiles of *Pseudomonas fluorescens* SBW25 reflects *in vitro* and *in planta* metabolic history. *Microb Ecol* **53**: 414–425.
- Huang WE, Ferguson A, Singer AC, Lawson K, Thompson IP, Kalin RM *et al.* (2009a). Resolving genetic functions within microbial populations: *in situ* analyses using rRNA and mRNA stable isotope probing coupled with single-cell Raman-fluorescence *in situ* hybridization. *Appl Environ Microbiol* **75**: 234–241.
- Huang WE, Griffiths RI, Thompson IP, Bailey MJ, Whiteley AS. (2004). Raman microscopic analysis of single microbial cells. *Anal Chem* **76**: 4452–4458.
- Huang WE, Li M, Jarvis RM, Goodacre R, Banwart SA. (2010). Shining light on the microbial world: the application of Raman microspectroscopy. *Adv Appl Microbiol* **70**: 153–186.
- Huang WE, Stoecker K, Griffiths R, Newbold L, Daims H, Whiteley AS *et al.* (2007b). Raman-FISH: combining stable-isotope Raman spectroscopy and fluorescence *in situ* hybridization for the single cell analysis of identity and function. *Environ Microbiol* **9**: 1878–1889.
- Huang WE, Ward AD, Whiteley AS. (2009b). Raman tweezers sorting of single microbial cells. *Environ Microbiol Rep* **1**: 44–49.
- Jardillier L, Zubkov MV, Pearman J, Scanlan DJ. (2010). Significant CO₂ fixation by small prymnesiophytes in the subtropical and tropical northeast Atlantic Ocean. *ISME J* **4**: 1180–1192.
- Karl DM. (2002). Microbiological oceanography - hidden in a sea of microorganisms. *Nature* **415**: 590–591.
- Krebs RA, Dunmire D, Partha R, Braiman MS. (2003). Resonance Raman characterization of proteorhodopsin's chromophore environment. *J Phys Chem B* **107**: 7877–7883.
- Lorenz P, Eck J. (2005). Metagenomics and industrial applications. *Nat Rev Microbiol* **3**: 510–516.
- Manefield M, Whiteley AS, Griffiths RI, Bailey MJ. (2002). RNA stable isotope probing, a novel means of linking microbial community function to phylogeny. *Appl Environ Microbiol* **68**: 5367–5373.
- Pandey A, Andersen JS, Mann M. (2000). Use of mass spectrometry to study signaling pathways. *Sci STKE* **2000**: pl1.
- Radajewski S, Ineson P, Parekh NR, Murrell JC. (2000). Stable-isotope probing as a tool in microbial ecology. *Nature* **403**: 646–649.
- Rimai L, Heyde ME, Gill D. (1973). Vibrational-spectra of some carotenoids and related linear polyenes - Raman spectroscopic study. *J Am Chem Soc* **95**: 4493–4501.
- Robert B. (2009). Resonance Raman spectroscopy. *Photosynth Res* **101**: 147–155.
- Stanier RY, Cohenbazire G. (1977). Phototropic prokaryotes - cyanobacteria. *Annu Rev Microbiol* **31**: 225–274.
- Stepanaukas R, Sieracki ME. (2007). Matching phylogeny and metabolism in the uncultured marine bacteria, one cell at a time. *Proc Natl Acad Sci USA* **104**: 9052–9057.
- Szalontai B, Gombos Z, Csizmadia V, Bagyinka C, Lutz M. (1994). Structure and interactions of phycocyanobilin chromophores in phycocyanin and allophycocyanin from an analysis of their resonance Raman spectra. *Biochemistry* **33**: 11823–11832.
- Tracewell CA, Cua A, Bocian DF, Brudvig GW. (2005). Resonance Raman spectroscopy of carotenoids in Photosystem II core complexes. *Photosynth Res* **83**: 45–52.
- Tracewell CA, Cua A, Stewart DH, Bocian DF, Brudvig GW. (2001). Characterization of carotenoid and chlorophyll photooxidation in photosystem II. *Biochemistry* **40**: 193–203.
- Tripp HJ, Bench SR, Turk KA, Foster RA, Desany BA, Niazi F *et al.* (2010). Metabolic streamlining in an open-ocean nitrogen-fixing cyanobacterium. *Nature* **464**: 90–94.
- Venter JC, Remington K, Heidelberg JF, Halpern AL, Rusch D, Eisen JA *et al.* (2004). Environmental genome shotgun sequencing of the Sargasso Sea. *Science* **304**: 66–74.
- Wagner M. (2009). Single-cell ecophysiology of microorganisms as revealed by Raman microspectroscopy or secondary ion mass spectrometry imaging. *Annu Rev Microbiol* **63**: 411–429.
- Weller R, Bateson MM, Heimbuch BK, Kopczynski ED, Ward DM. (1992). Uncultivated cyanobacteria, chloroflexus-like inhabitants, and spirochete-like inhabitants of a hot-spring microbial mat. *Appl Environ Microbiol* **58**: 3964–3969.
- Wu HW, Volponi JV, Oliver AE, Parikh AN, Simmons BA, Singh S. (2011). *In vivo* lipidomics using single-cell Raman spectroscopy. *Proc Natl Acad Sci USA* **108**: 3809–3814.
- Zehr JP, Bench SR, Carter BJ, Hewson I, Niazi F, Shi T *et al.* (2008). Globally distributed uncultivated oceanic N₂-fixing cyanobacteria lack oxygenic photosystem II. *Science* **322**: 1110–1112.
- Zhang JW. (2011). The diversity and biotechnological application of marine microbes producing Omega-3 fatty acids. PhD thesis, Newcastle University: Newcastle upon Tyne, UK.

Supplementary Information accompanies the paper on The ISME Journal website (<http://www.nature.com/ismej>)